FULL PAPER

Dalton
www.rsc.org/dalton

Chiral discrimination in the formation reaction and at equilibrium for *N*,*N*,*N*′,*N*′-tetramethyl-1,2-diaminocyclohexane–PtG_2 complexes

Michele Benedetti,[a] Jamil S. Saad,[b] Luigi G. Marzilli[c] and Giovanni Natile*[d]

[a] *Dipartimento di Scienze e Tecnologie Biologiche ed Ambientali, Università degli Studi di Lecce, Via Monteroni, I-73100 Lecce, Italy*

[b] *Howard Hughes Medical Institute and Department of Chemistry and Biochemistry University of Maryland, Baltimore County, 1000 Hilltop Circle Baltimore, MD 21250, USA*

[c] *Department of Chemistry, Louisiana State University, Baton Rouge, LA 70803, USA*

[d] *Dipartimento Farmaco-Chimico, Università degli Studi di Bari, Via E. Orabona 4, I-70125 Bari, Italy. E-mail: natile@farmchim.uniba.it*

Received 28th October 2002, Accepted 20th December 2002
First published as an Advance Article on the web 3rd February 2003

The effect of an extremely bulky carrier ligand, such as *N*,*N*,*N*′,*N*′-tetramethyl-1,2-diaminocyclohexane (**Me_4DACH**, *R*,*R* and *S*,*S* configurations of the asymmetric carbon atoms of the chelate ring), upon the rate of formation and stability of **Me_4DACH**–Pt**G_2** derivatives has been investigated (**G** = 9-EtG, 3′-GMP, and 5′-GMP). Of the three possible rotamers, two head-to-tail (ΔHT and ΛHT) and one head-to-head (HH), only the former two are found in solution. The very small difference in H8 chemical shifts between ΔHT and ΛHT rotamers indicates that the relationship between the two guanines is very similar in the two conformers which are canted to the same degree but in opposite directions. A smaller interligand steric clash appears to favour the HT rotamer in which the H8 atoms of the guanines are on the same side of pseudo-axial N–Me's with respect to the platinum coordination plane. In the case of 5′-GMP, because of the absence of aminic protons on the carrier ligand, the 5′-phosphate directs its H-bonding potential towards the second ligand in *cis*-position (the coordinated H_2O molecule in the mono adduct, [**Me_4DACH**–Pt(H_2O)(5′-GMP)]$^+$, and the *cis*-**G** in the bis-adduct). As a consequence the rotamer in which such an interaction is possible, with the nucleotide keeping its favoured *anti* conformation, is more stable than expected. In contrast with the behaviour of 5′-GMP, 3′-GMP is found to increase the reactivity of the mono adduct in which the phosphate is directed towards the *cis*-water molecule and to give a negligible contribution to the stability of the HT rotamer in which the 3′-phosphate is directed towards the *cis*-nucleotide.

Introduction

The serendipitous discovery by Rosenberg of the antitumoral activity of cisplatin (*cis*-[$PtCl_2(NH_3)_2$])[1–3] over twenty years ago has represented a breakthrough in the chemotherapy of tumors.[4]

In the following years, thousands of new platinum compounds have been synthesised and tested for anti-tumor activity. Some dozens have entered human clinical trials[5] and one, the diamine(1,1-cyclobutanedicarboxylato-*O*,*O*′)-platinum(II) (carboplatin), has achieved world-wide approval and routine clinical use, due to a lower toxicity compared to cisplatin. Unfortunately, carboplatin is active in the same range of tumors as cisplatin. More recently two other platinum compounds have received limited approval for use in some countries: diammine(glycolato-*O*,*O*′)platinum(II) (nedaplatin or 254-S) and (*R*,*R*)-1,2-diaminocyclohexane(oxalato-*O*,*O*′)-platinum(II) (oxaliplatin or L-OHP).[6]

Cisplatin targets DNA mostly by binding to N7 of adjacent purines.[6–10] This intrastrand adduct is thought to be the lesion responsible for cell death, but the mechanism of action is not entirely understood. The activity of *cis*-PtA_2X_2 compounds was found to decrease in the series A = NH_3 > RNH_2 > R_2NH.[11] This correlation with the number of amine hydrogens led to speculation about hydrogen-bond formation between the amine NH's and a nucleotide-phosphate or a guanine-O6 of the cross-link.[10–12]

In order to investigate the effect of substituents on the amine carrier ligand upon the interaction of platinum drugs with DNA bases, diamine ligands having C_2 symmetry and one alkyl substituent and one hydrogen on each coordinated nitrogen, were selected. Moreover, the stereochemistry of the carrier ligand was preorganized by introducing chiral carbon centres in the chain linking the two nitrogens. These ligands were termed Chirality Controlling Chelates (**CCC**) because they induced a marked preference for either the ΔHT or the ΛHT conformer in **CCC**-Pt**G_2** derivatives (Scheme 1, the configurations at the chelate ring atoms of the **CCC** ligand are given in parentheses, **G_2** stands for two untethered guanine bases. The guanine bases are indicated with arrows, the head of the arrow pointing in the direction of H8. HT stands for Head-to-Tail orientation of the coordinated nucleobases, Λ or Δ chirality of the HT conformers is defined by the chirality of two screw lines, one perpendicular to the coordination plane and passing through the platinum centre and the other connecting the O6 atoms of the two guanines).[13–21] The preference mentioned above is mediated by two requirements: the minimization of steric interactions between each **G** and the alkyl substituent on the *cis* nitrogen and the preference of the HT rotamer for the conformation that accommodates the two guanines in a "6-in" conformation (the 6-membered ring of each guanine leaning towards the *cis*-**G**), the "6-in" conformation ensuring a better internucleotide dipole–dipole interaction. The combination of these two effects results in the *R* configuration of the aminic nitrogens favouring a right hand canting of the nucleobases and stabilizing the ΔHT rotamer, the *S* configuration favouring a left hand canting of the nucleobases and stabilizing the ΛHT conformer. Right- and left-hand canting is defined by the chirality of two screw lines, one passing through the two N7 atoms of the coordinated guanines and the other passing through H8 and bisecting a given guanine.

Having understood the critical role of N-alkyl groups in influencing the stereochemistry of coordinated nucleotides, we have extended the investigation to carrier ligands analogous to

DOI: 10.1039/b210616g

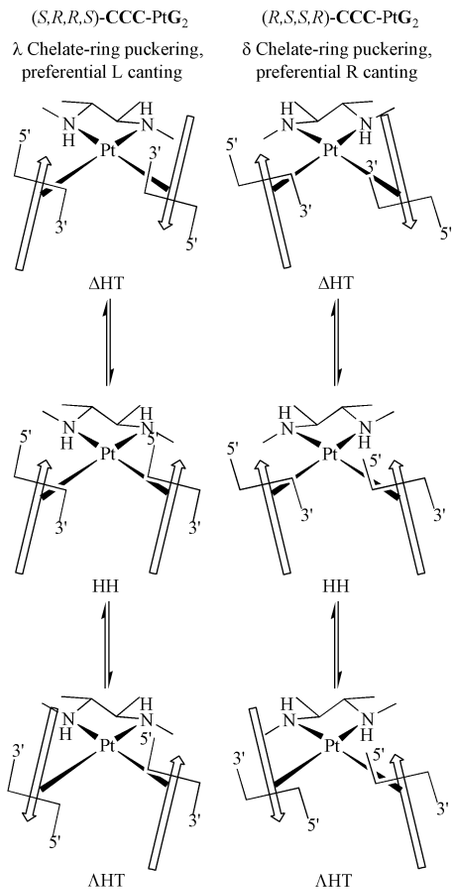

Scheme 1

the **CCC** ligands previously investigated but having two methyl substituents on each N-donor. Therefore, in this paper we will examine the case of *N*,*N*,*N*′,*N*′-tetramethyl-1,2-diaminocyclohexane having *R*,*R* and *S*,*S* configurations at the asymmetric carbons.

Results

The reactions were investigated by CD and ^{1}H NMR spectroscopy. NMR and CD spectra were registered simultaneously (within 10–15 min) so that it was possible to correlate each CD spectrum to a given conformer composition deduced from integration of the NMR signals.

(*R*,*R*)-Me$_4$DACH–PtG$_2$ complexes

G = 9-EtG. The ^{1}H NMR spectrum (22 °C) of a solution containing [(*R*,*R*)-**Me$_4$DACH**–Pt(D$_2$O)$_2$]$^{2+}$ and 9-EtG (molar ratio 1 : 2) exhibits four new H8 peaks 1 h after mixing. Two signals of comparable intensities are close to 8.55 ppm and two signals are at 8.24 and 8.27 ppm, respectively (Fig. 1). During the course of the reaction there is a steady decrease of the H8 peak of free 9-EtG and a steady increase of the H8 peaks at 8.24 and 8.27 ppm. The H8 peaks close to 8.55 ppm first grow to a maximum intensity and than decrease to zero.

The time dependence of the peaks close to 8.55 ppm indicates that they belong to the mono-adduct [(*R*,*R*)-**Me$_4$DACH**–Pt(D$_2$O)(9-EtG)]$^{2+}$. Because of the C_2 symmetry of the **Me$_4$DACH** ligand, the observation of two sets of resonances for the mono-adduct can only arise from the formation of two rotamers. Scheme 2 shows sketches of the mono-adduct with the **Me$_4$DACH** placed in the rear and the **G** nucleobase placed on the left-hand coordination site, the configurations at the chelate ring carbon atoms are given in parentheses. The two rotamers of the mono adducts have been defined in relation to the type of HT conformer (Λ or Δ) which is formed by coordination of a

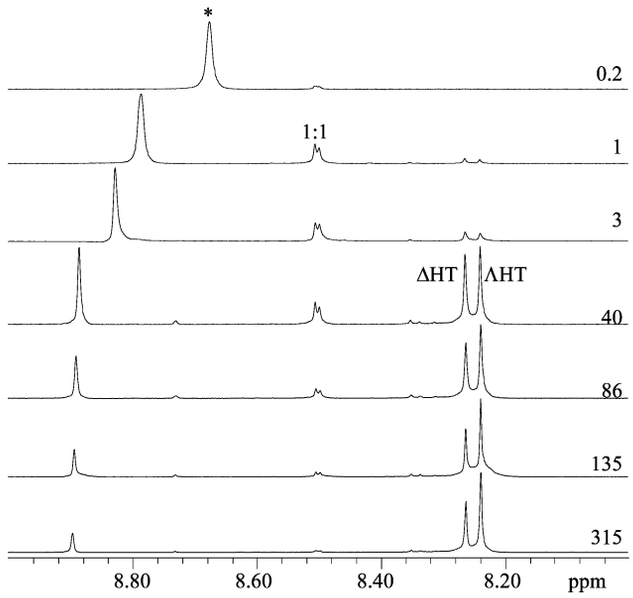

Fig. 1 Reaction of [(*R*,*R*)-**Me$_4$DACH**–Pt(D$_2$O)$_2$]$^{2+}$ with 9-EtG at pH* < 3 and 22 °C. ^{1}H NMR spectra were taken at different time intervals (hours, as indicated on each spectrum). Peaks of free 9-EtG (asterisk), mono-adduct (1 : 1), and bis-adduct (ΔHT and ΛHT) are labeled. The shift of the H8 resonance of the free 9-EtG with time is due to the increase in acidity consequent on the decreasing concentration of free base.

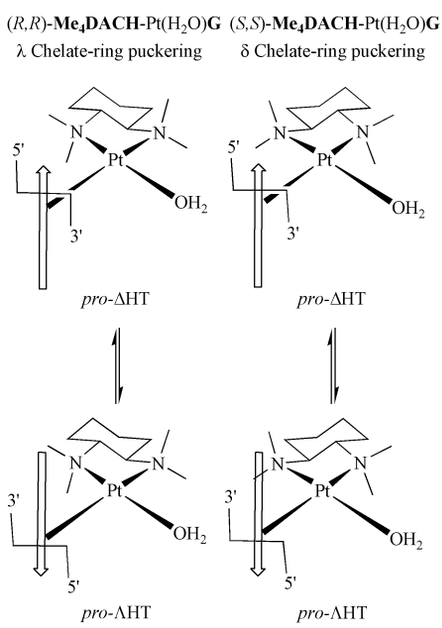

Scheme 2

second **G** base (in place of the water molecule) in a head-to-tail orientation with respect to the pre-existing **G**. The intensity ratio between the two signals close to 8.55 ppm did not change with time, indicating that the rotamer composition of the mono-adduct is under thermodynamic control.

The two signals at 8.24 and 8.27 ppm are assigned to the bis-adduct [(*R*,*R*)-**Me$_4$DACH**–Pt(9-EtG)$_2$]$^{2+}$. Three rotamers of the 2 : 1 adduct can be formed: two head to tail (ΛHT and ΔHT) and one head-to-head (HH), as already shown in Scheme 1 for **CCC** ligands (in the case of **Me$_4$DACH**, however, a second Me takes the place of the proton on each nitrogen). Each HT rotamer (C_2 symmetry) will give one H8 and two N–CH$_3$ ^{1}H NMR signals. The two N–CH$_3$ signals include one for the pseudo-axial and the other for the pseudo-equatorial methyls. For the HH rotamer (C_1 symmetry), the two **G**'s are not equivalent, therefore two H8 (of equal intensities) and four N–CH$_3$ signals (also of equal intensities) are expected. The two H8

Table 1 ^{1}H chemical shifts, ppm downfield TSP (TSP = sodium 3-(trimethylsilyl)propionate-2,2,3,3-d_4, $^3J_{H-H}$ in Hz are given in square brackets) and conformer percentages in the first stage of the reaction (2–3 h, $(\%)_{kin}$) and at equilibrium (7–25 d, $(\%)_{therm}$) for **Me_4DACH**–Pt**G_2** complexes[a]

Complex	Conformer	H8	H1′	NMe_2	$(\%)_{kin}$	$(\%)_{therm}$
(*R*,*R*)-**Me_4DACH**–Pt(9-EtG)$_2$	ΛHT	8.24		2.91, 2.62	46	63
	ΔHT	8.27		2.78, 2.75	54	37
(*S*,*S*)-**Me_4DACH**–Pt(9-EtG)$_2$	ΛHT	8.26		2.78, 2.76	54	39
	ΔHT	8.24		2.92, 2.63	46	61
(*R*,*R*)-**Me_4DACH**–Pt(3′-GMP)$_2$	ΛHT	8.46	5.88 [4.5]	2.92, 2.65	45	60
	ΔHT	8.53	5.93 [4]	2.82, 2.78	55	40
(*S*,*S*)-**Me_4DACH**–Pt(3′-GMP)$_2$	ΛHT	8.48	5.88 [4.5]	2.80, 2.75	47	40
	ΔHT	8.52	5.92 [4]	2.93, 2.66	53	60
(*R*,*R*)-**Me_4DACH**–Pt(5′-GMP)$_2$	ΛHT	8.42	5.86 [6]	2.94, 2.70	19	73
	ΔHT	8.44	5.89 [6]	2.82, 2.78	81	27
(*S*,*S*)-**Me_4DACH**–Pt(5′-GMP)$_2$	ΛHT	8.45	5.87 [6]	2.84, 2.79	43	59
	ΔHT	8.39	5.85 [6]	2.93, 2.66	57	41

[a] Solvent D_2O, pH in the range 1.7–2.8.

signals at 8.24 and 8.27 ppm have unequal intensities, therefore they must belong to the two HT rotamers. There are no signals of equal intensity assignable to the HH rotamer, indicating that the HH conformer does not form.

One HT conformer of the bis-adduct (H8 at 8.27 ppm) is initially slightly more abundant than the other (H8 at 8.24 ppm). The CD of the corresponding solution has positive Cotton effects at 208 and 250 nm and negative Cotton effects at 220 and 285 nm (Fig. 2). With time, the initially more abundant conformer decreases and, at equilibrium, becomes less abundant. Correspondingly, an inversion of the CD bands is observed (the Cotton effects become negative at 204 and 250 nm and positive at 222 and 285 nm).

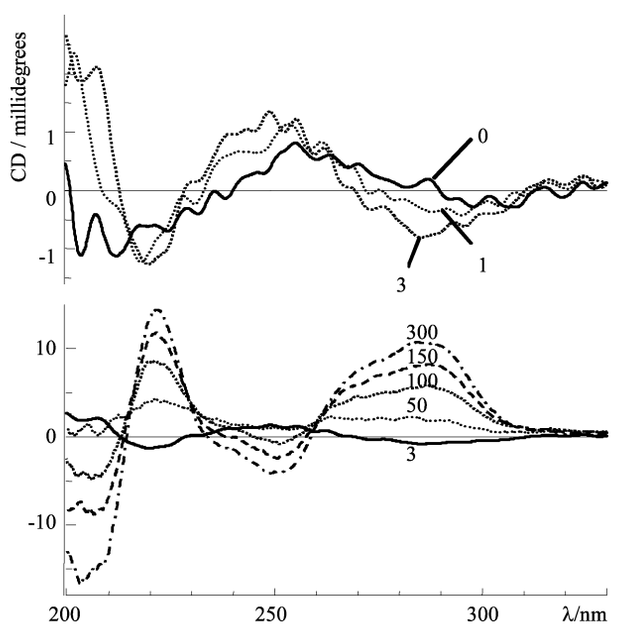

Fig. 2 Reaction of [(*R*,*R*)-**Me_4DACH**–Pt$(D_2O)_2]^{2+}$ with 9-EtG at pH* < 3 and 22 °C. CD spectra were taken at different time intervals (hours, as indicated on each curve).

Common CD features of previously studied *cis*-PtA_2**G_2** adducts led us to conclude that HT conformers make the greatest contribution to the CD spectrum [14,15,19,22] and that HT conformers of opposite chirality (Λ or Δ) also have opposite CD features. Moreover, the CD spectrum of a mixture of conformers is reflective of the dominant conformer in solution. Therefore, in the present case the CD spectra (Fig. 2) indicate a preference for the ΔHT rotamer in the first steps of the reaction and a preference for the ΛHT rotamer at equilibrium (Table 1).

G = 3′-GMP. The reaction course of [(*R*,*R*)-**Me_4DACH**–Pt$(D_2O)_2]^{2+}$ with 3′-GMP (molar ratio 1 : 2) was similar to that already described for the 9-EtG case. The two conformers of the mono-adduct, [(*R*,*R*)-**Me_4DACH**–Pt(D_2O)(3′-GMP)]$^+$, have H8 signals of comparable size at 8.75 and 8.73 ppm, whereas the two HT conformers of the bis-adduct, (*R*,*R*)-**Me_4DACH**–Pt(3′-GMP)$_2$, have H8 signals of unequal intensities at 8.46 and 8.54 ppm. ^{1}H NMR and CD spectra (Fig. 3 and 4) are in accord with the prevalence of the ΔHT conformer in the initial stage of the reaction (up to 17 h) and with a prevalence of the ΛHT rotamer at equilibrium (17 days).

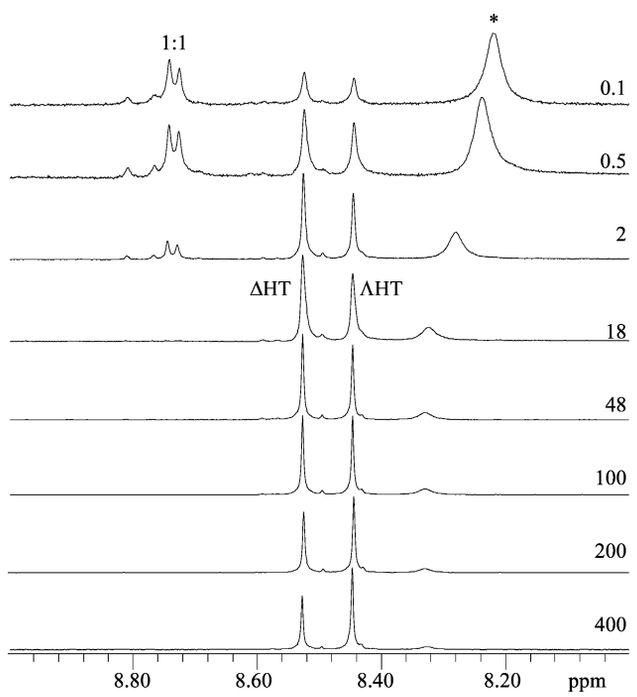

Fig. 3 Reaction of [(*R*,*R*)-**Me_4DACH**–Pt$(D_2O)_2]^{2+}$ with 3′-GMP at pH* < 3 and 22 °C. ^{1}H NMR spectra were taken at different time intervals (hours, as indicated on each spectrum). Peaks of free 3′-GMP (asterisk, the shift with time is due to the increase in acidity consequent on the decreasing concentration of free base), mono-adduct (1 : 1), and bis-adduct (ΔHT and ΛHT) are labeled.

G = 5′-GMP. The ^{1}H NMR spectra (22 °C) of a solution containing [(*R*,*R*)-**Me_4DACH**–Pt$(D_2O)_2]^{2+}$ and 5′-GMP (molar ratio 1 : 2) contained 3 new peaks in the H8 region 1 h after mixing (Fig. 5).

One signal (at 8.72 ppm) is in the region of the mono-adducts and is accompanied by two doublets of comparable size in the region of H1′. Thus, this set of signals is assigned to the [(*R*,*R*)-**Me_4DACH**–Pt(D_2O)(5′-GMP)]$^+$ mono-adduct for which the two conformers have overlapping H8 signals. The two H8 signals at 8.41 and 8.44 ppm have very different intensities and are assigned to the two HT conformers of the (*R*,*R*)-**Me_4DACH**–

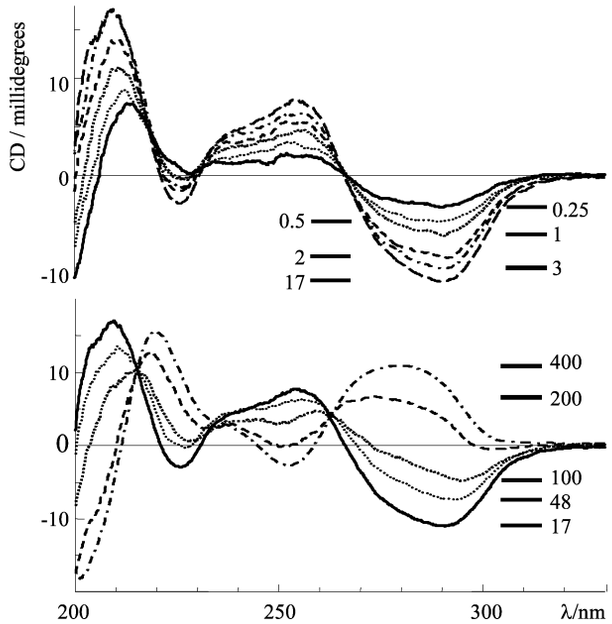

Fig. 4 Reaction of $[(R,R)$-**Me$_4$DACH**–Pt$(D_2O)_2]^{2+}$ with 3′-GMP at pH* < 3 and 22 °C. CD spectra were taken at different time intervals (hours, as indicated on each spectrum).

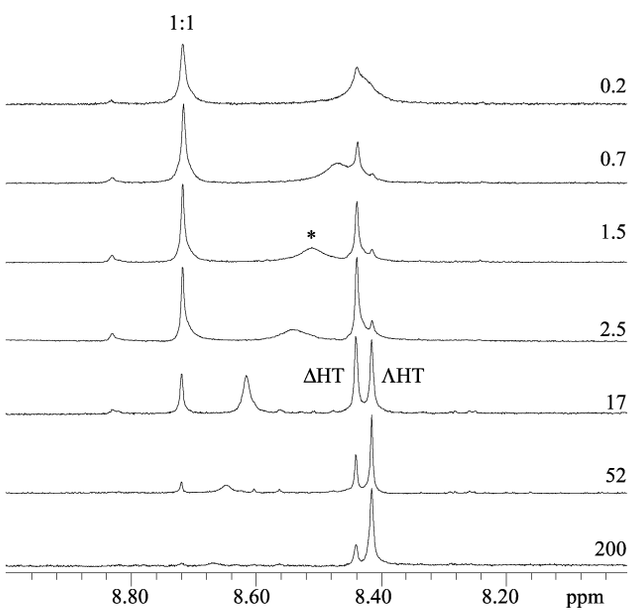

Fig. 5 Reaction of $[(R,R)$-**Me$_4$DACH**–Pt$(D_2O)_2]^{2+}$ with 5′-GMP at pH* < 3 and 22 °C. ^{1}H NMR spectra were taken at different time intervals (hours, as indicated on each spectrum). Peaks of free 5′-GMP (asterisk, the shift with time is due to the increase in acidity consequent on the decreasing concentration of free base), mono-adduct (1 : 1), and bis-adduct (ΔHT and ΛHT) are labeled.

Pt$(5'$-GMP$)_2$ bis-adduct. The peaks of the mono-adduct reach the highest intensities 3 h after mixing and then decrease to zero. In the early stage of the reaction the signal of the HT conformer at 8.44 ppm is far more intense than the signal of the HT conformer at 8.41 ppm. After allowing for the thermodynamic equilibrium to be established (26 days), the signal at 8.41 ppm, initially less intense, becomes much more intense than the signal at 8.44 ppm which was initially more favoured.

The CD spectra show during the first stage of the reaction positive Cotton effects at 209 and 255 nm and negative Cotton effects at 220 and 285 nm. Subsequently, while the interconversion between the two rotamers of the bis-adduct leads to the equilibrium composition (26 days), the Cotton effects change sign (Fig. 6). As for the case of 9-EtG and 3′-GMP, for 5′-GMP

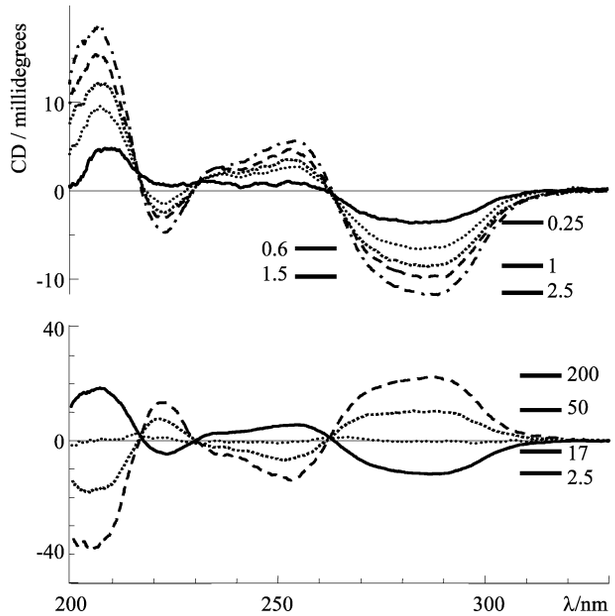

Fig. 6 Reaction of $[(R,R)$-**Me$_4$DACH**–Pt$(D_2O)_2]^{2+}$ with 5′-GMP at pH* < 3 and 22 °C. CD spectra were taken at different time intervals (hours, as indicated on each spectrum).

also the CD spectra are in accord with a prevalence of the ΔHT rotamer in the first stage of the reaction, and a prevalence of the ΛHT rotamer at equilibrium.

(S,S)-Me$_4$DACH–PtG$_2$ Complexes

G = 9-EtG. NMR and UV-VIS spectra of a solution containing $[(S,S)$-**Me$_4$DACH**–Pt$(D_2O)_2]^{2+}$ and 9-EtG (in a molar ratio 1 : 2) were similar to those observed for the analogous reaction with the enantiomeric species $[(R,R)$-**Me$_4$DACH**–Pt$(D_2O)_2]^{2+}$. However, the CD spectra showed inverted signs: positive bands at 220 and 285 nm and negative bands at 205 and 250 nm for the first 3 h after mixing of the reactants (predominance of the ΛHT rotamer) negative bands at 220 and 285 nm and positive bands at 205 and 250 nm in the following 13 days (predominance of the ΔHT rotamer at equilibrium).

G = 3′-GMP. The ^{1}H NMR spectra (22 °C) of a solution containing $[(S,S)$-**Me$_4$DACH**-Pt$(D_2O)_2]^{2+}$ and 3′-GMP in the molar ratio of 1 : 2 are shown in Fig. 7 for different reaction times. The H8 signal at 8.74 ppm and the H1′ doublets, of similar size, at 6.03 and 6.04 ppm (not shown) are assigned to two conformers of the $[(S,S)$-**Me$_4$DACH**–Pt$(D_2O)(3'$-GMP$)]^+$ mono-adduct. The two H8 signals at 8.48 and 8.52 ppm and the corresponding H1′ doublets at 5.88 and 5.92 ppm (Table 1) are assigned to the two HT rotamers of the (S,S)-**Me$_4$DACH**–Pt$(3'$-GMP$)_2$ bis-adduct. The predominance of the H8 peak at 8.52 ppm (with respect to that at 8.48 ppm) is very slight in the early stage of the reaction and increases with time. Correspondingly, the Cotton effects, initially very weak, increase with time and always have the typical features of the ΔHT rotamer (Fig. 8). Therefore, differently from the case of 9-EtG just described, 3′-GMP appears to favour the ΔHT rotamer from the early stage of the reaction up to the end.

G = 5′-GMP. The ^{1}H NMR spectra (22 °C) of a solution containing $[(S,S)$-**Me$_4$DACH**–Pt$(D_2O)_2]^{2+}$ and 5′-GMP (molar ratio 1 : 2) are shown in Fig. 9 for different reaction times. Two signals, having very close chemical shifts (8.72 and 8.73 ppm), and an intensity ratio of *ca.* 2 : 1, fall in the region of the mono-adducts and are assigned to $[(S,S)$-**Me$_4$DACH**–Pt$(D_2O)(5'$-GMP$)]^+$. The corresponding doublets in the region of H1′ protons fall at 6.03 and 6.06 ppm (not shown). This is

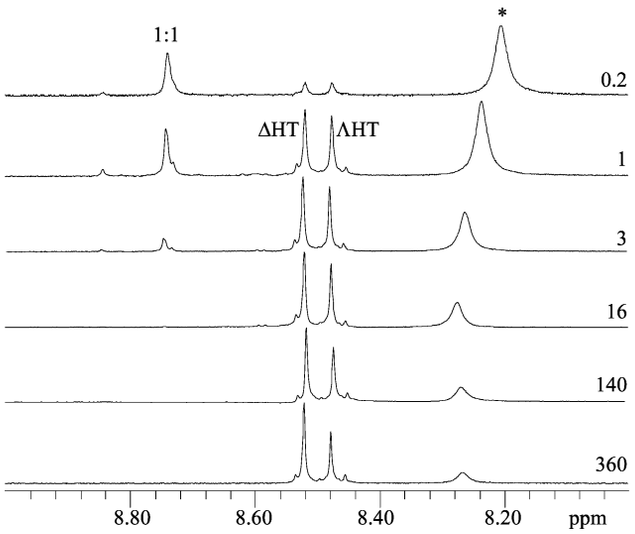

Fig. 7 Reaction of $[(S,S)$-**Me$_4$DACH**–Pt$(D_2O)_2]^{2+}$ with 3′-GMP at pH* < 3 and 22 °C. ^{1}H NMR spectra were taken at different time intervals (hours, as indicated on each spectrum). Peaks of free 3′-GMP (asterisk, the shift with time is due to the increase in acidity consequent on the decreasing concentration of free base), mono-adduct (1 : 1), and bis-adduct (ΔHT and ΛHT) are labeled. The small peaks flanking the two signals of the bis-adduct belong to a small amount of the (R,R)-**Me$_4$DACH**–Pt**G$_2$** complex present as impurity.

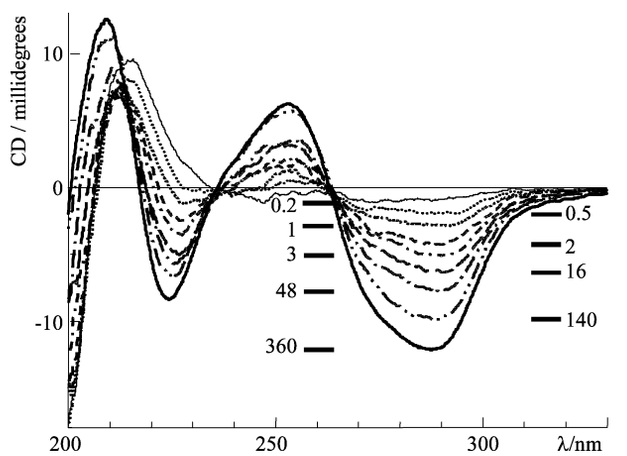

Fig. 8 Reaction of $[(S,S)$-**Me$_4$DACH**–Pt$(D_2O)_2]^{2+}$ with 3′-GMP at pH* < 3 and 22 °C. CD spectra were taken at different time intervals (hours, as indicated on each spectrum).

the only case in which the two conformers of the mono-adduct are present in a molar ratio quite different from 1. The other two H8 signals (at 8.39 and 8.45 ppm) accompanied by doublets in the region of H1′ signals (at 5.85 and 5.87 ppm, respectively, see Table 1) have different intensities and are assigned to the two HT conformers of the (S,S)-**Me$_4$DACH**–Pt$(5'$-GMP$)_2$ bis-adduct. The peak at 8.45 ppm is initially less intense than that at 8.39 ppm (ratio of *ca.* 0.75) but becomes the most intense at equilibrium (ratio of *ca.* 1.4).

The CD spectra show in the early stage of the reaction (highest intensities after 12 h) positive Cotton effects at 206 and 253 nm and negative Cotton effects at 223 and 290 nm. For longer times the Cotton effects first decrease and then invert sign, reaching the highest intensities after 24 days when the thermodynamic equilibrium is established (Fig. 10). Therefore, the CD spectra indicate a prevalence of the ΔHT rotamer in the early stages of the reaction and a prevalence of the ΛHT rotamer at equilibrium. Such behaviour is different from that observed in the cases of 9-EtG (prevalence of the ΛHT rotamer at short reaction time and of the ΔHT rotamer at equilibrium) and of 3′-GMP (prevalence of the ΔHT rotamer from the beginning up to the end of the reaction).

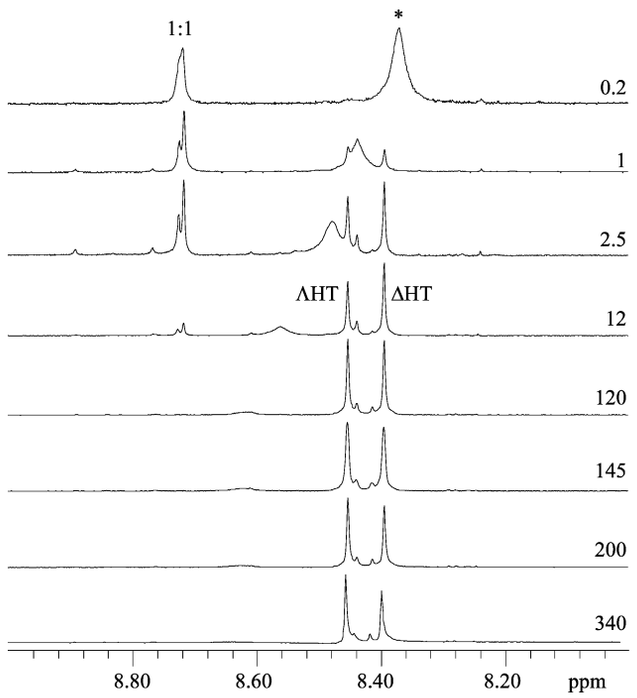

Fig. 9 Reaction of $[(S,S)$-**Me$_4$DACH**–Pt$(D_2O)_2]^{2+}$ with 5′-GMP at pH* < 3 and 22 °C. ^{1}H NMR spectra were taken at different time intervals (hours, as indicated on each spectrum). Peaks of free 5′-GMP (asterisk, the shift with time is due to the increase in acidity consequent on the decreasing concentration of free base), mono-adduct (1 : 1), and bis-adduct (ΔHT and ΛHT) are labeled. The small peaks in between the two signals of the bis-adduct belong to a small amount of the (R,R)-**Me$_4$DACH**–Pt$(5'$-GMP$)_2$ complex present as impurity.

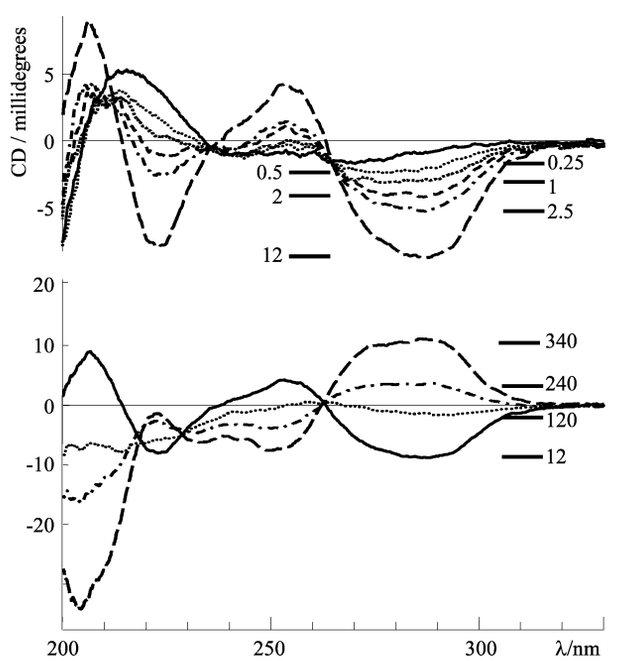

Fig. 10 Reaction of $[(S,S)$-**Me$_4$DACH**–Pt$(D_2O)_2]^{2+}$ with 5′-GMP at pH* < 3 and 22 °C. CD spectra were taken at different time intervals (hours, as indicated on each spectrum).

Discussion

Chemical shifts of H8 and N–Me's

In previous investigations concerning with (**CCC**)-Pt**G$_2$** complexes, the difference in chemical shift between the H8 signals of the ΛHT and ΔHT rotamers was of the order of 0.2–0.3 ppm.[13–15,18,21] In the complexes with the tetramethylated diamines here considered, the chemical shift difference between

the H8 signals of the ΛHT and ΔHT rotamers is in the range of 0.02–0.08 ppm, Table 1.

The major contribution to the difference in H8 chemical shifts in (**CCC**)-Pt**G**$_2$ complexes stems from the location of the H8 protons with respect to the shielding cone of the *cis*-guanine. HT rotamers tend to be canted in order to assume a "6-in" conformation. The canting of the nucleobases, however, is also influenced by the steric repulsion between the **G** and the alkyl substituent on the *cis*-amine. Therefore the canting will be greater (and the H8 less shielded) when the HT chirality and the carrier ligand chirality both favour the same direction of canting (*R* chirality of the *cis* nitrogen and Δ chirality of the HT rotamer or *S* chirality of the *cis* nitrogen and Λ chirality of the HT rotamer).

In the present investigation the chemical shift difference between the H8 protons of the Δ and ΛHT conformers is very small indicating that either the degree of canting is also very small for both rotamers or, unlike the case of **CCC** ligands, for a given chirality of the **Me$_4$DACH** ligand, the two HT rotamers are canted to the same degree but in opposite directions. Both hypotheses are plausible and don't exclude each other. The four methyl substituents at the aminic nitrogens, symmetrically distributed on both sides of the coordination plane, could limit the degree of canting of the guanine bases and have little effect upon the canting directionality of the nucleobases.

In the N–Me region four signals (two for each rotamer) were observed (Table 1). The chemical shift difference between geminal N–Me's is in the range of 0.25–0.30 ppm when the 6-membered ring of the *cis*-guanine is on the same side of the pseudo-equatorial N–Me with respect to the platinum coordination plane. The difference drops to 0.02–0.05 ppm when the 6-membered ring of the *cis*-guanine is on the same side of the pseudo-axial N–Me with respect to the platinum coordination plane. Before coordination of the **G** bases the chemical shift of each N–Me is dominated by the magnetic anisotropy of the platinum centre, hence a pseudo-equatorial N–Me, being closer to the coordination plane, will be more shielded than a pseudo-axial N–Me. After coordination of the **G** bases each N–Me is also affected by the magnetic anisotropy of the *cis*-**G**. When the 6-membered ring of the *cis*-**G** is on the same side of a pseudo-equatorial N–Me, with respect to the platinum coordination plane, the high-field pseudo-equatorial N–Me will be further shielded by the magnetic field of the guanine and the chemical shift separation between pseudo-equatorial and pseudo-axial N–Me's will be larger. In contrast, when the 6-membered ring of the guanine is on the same side of a pseudo-axial N–Me, the low-field signal of the pseudo-axial N–Me will be shifted upfield by the *cis*-**G** and, as a consequence, the separation in chemical shift between pseudo-equatorial and pseudo-axial N–Me's will be smaller. The fact that the average chemical shift of the N–Me's is nearly coincident for the two HT rotamers indicates that the shielding effect by the *cis*-guanine is very similar for pseudo-equatorial and pseudo-axial N–Me's.

Chiral discrimination at equilibrium for Me$_4$DACH–PtG$_2$ complexes

In most of the cases presently investigated the HT rotamer which is favoured at equilibrium has a chirality different from that of the HT rotamer favoured in the formation reaction. The composition at equilibrium reflects the different stabilities of the two HT rotamers as determined by interligand interactions. In contrast, the composition in the formation reaction reflects the different kinetic preference for one or the other HT conformer. We will discuss the two cases separately.

For the 9-EtG and 3′-GMP derivatives the rotamer which is favoured at equilibrium has the ΛHT conformation in the case of (*R*,*R*)-**Me$_4$DACH** and the ΔHT conformation in the case of (*S*,*S*)-**Me$_4$DACH**. Thus, the rotamer which is favoured at equilibrium has the same conformation as found in analogous complexes with **CCC** ligands having similar chiralities at the asymmetric carbons bridging the two nitrogens.[14,15,19] In complexes with **CCC** ligands the degree of canting is greater for one HT rotamer (the more stable) than for the other because in the former case the H8 atom of each guanine is on the side of the NH of the *cis*-amine with respect to the platinum coordination plane while in the latter case the H8 of each guanine is on the side of the N-alkyl group of the *cis*-amine and steric interaction between the two groups limits the degree of canting for a "6-in" conformation. For **Me$_4$DACH** complexes we observe that the preferred HT rotamers have the H8 atom of the *cis*-guanine on the same side of the pseudo-axial N–Me with respect to the coordination plane. Pseudo-axial methyl groups protrude slightly less towards the *cis*-ligands than the pseudo-equatorial methyls; therefore they could leave more space for accommodating the guanine H8 atoms of a "6-in" conformer.

In previous investigations dealing with **CCC** ligands it was also found that, in the case of 3′-GMP derivatives, the ΔHT rotamer is stabilised by phosphate-N1H *cis*-**G** internucleotide interactions.[19,22,23] In the present case such a phosphate-N1H *cis*-**G** interaction does not appear to give any significant contribution to the stability of the ΔHT rotamer at equilibrium. In fact for a given chirality of the **Me$_4$DACH** ligand the percentage of the ΔHT rotamer is similar for the 3′-GMP and the 9-EtG derivatives although for the latter compound such a phosphate-N1H *cis*-**G** interaction is not possible. Moreover similar percentages are also observed for ΛHT and ΔHT rotamers of **Me$_4$DACH**-Pt(3′-GMP)$_2$ complexes of opposite chiralities. It is conceivable that the steric bulk created by the carrier ligand with fully substituted N-donors imposes on the coordinated nucleotides steric restrictions that do not allow formation of internucleotide 3′-phosphate-N1H *cis*-**G** H-bond interactions.

For the 5′-GMP derivative, the rotamer which is favoured at equilibrium has always the ΛHT conformation independently from the *R*,*R* or *S*,*S* configuration of the **Me$_4$DACH** ligand. Moreover, the preference for the ΛHT rotamer is greater for (*R*,*R*)-**Me$_4$DACH** than for (*S*,*S*)-**Me$_4$DACH**. In the *R*,*R* system the abundance of the ΛHT rotamer is far greater than that observed in the corresponding compounds with 9-EtG and 3′-GMP, thus there must be an additional stabilizing factor for this rotamer. Most probably the additional factor is a phosphate-N1H *cis*-**G** H-bond interaction (in ΛHT the 5′-phosphate of each guanine is directed towards the *cis*-**G**, assuming an *anti* conformation for the nucleotide). This type of interaction was already postulated for similar complexes in the case of **CCC** ligands.[19,22,23] The same 5′-phosphate-N1H *cis*-**G** interaction can be invoked to explain the greater abundance of the ΛHT rotamer found in the case of (*S*,*S*)-**Me$_4$DACH**. In this case the 5′-phosphate-N1H *cis*-**G** interaction is such to counterbalance the destabilization of the HT rotamer having the H8 atoms of the guanines on the same side of the pseudo-axial N–Me's.

Chiral discrimination in the formation reaction

In the case of 9-EtG, NMR and CD spectra indicate that in the formation reaction the preferred rotamer has ΔHT conformation in the case of (*R*,*R*)-**Me$_4$DACH** and ΛHT conformation in the case of (*S*,*S*)-**Me$_4$DACH** (Table 1). Opposite conformations were favoured at equilibrium. The kinetic preference for a given HT rotamer could stem from a slightly greater reactivity of the corresponding mono-adduct: *pro*-ΔHT in the case of (*R*,*R*)-**Me$_4$DACH** and *pro*-ΛHT in the case of (*S*,*S*)-**Me$_4$DACH** (Scheme 2). Both mono-adducts have the H8 atom of the guanine on the same side of a pseudo-equatorial *cis*-N–Me and it has been hypothesized in the previous section that in this case the canting is smaller. A less canted guanine could leave more space to the incoming second molecule of nucleobase.

An unexpected behavior was observed in the case of 3′-GMP. In both the (*R*,*R*) and (*S*,*S*)-**Me$_4$DACH** systems the ΔHT rotamer was preferred in the formation reaction, indicating a greater reactivity of the *pro*-ΔHT mono-adduct. By analogy with the 9-EtG case, a greater reactivity of the *pro*-ΔHT mono-adduct was expected only for (*R*,*R*)-**Me$_4$DACH** but not for (*S*,*S*)-**Me$_4$DACH**. A possible explanation for this unusual behavior is that the *pro*-ΔHT monofunctional adduct increases its reactivity because it has the 3′-phosphate directed towards the solvated *cis*-coordination position (assuming an *anti* conformation of the nucleotide) and can offer an anchimeric assistance either to the release of the water molecule or to the entering of the second molecule of nucleotide. An increased reactivity of the mono-adduct is also in accord with the faster rate of formation of the bis-adduct observed with 3′-GMP than with 9-EtG.

In the case of 5′-GMP, as in the case of 3′-GMP, the ΔHT rotamer was again the preferred species in the formation reaction for both the (*R*,*R*) and (*S*,*S*)-**Me$_4$DACH** systems. Moreover, for the (*R*,*R*)-**Me$_4$DACH** system the kinetic preference for the ΔHT rotamer was much greater than that observed for 9-EtG and 3′-GMP. The overall behavior can be accounted for by assuming a reduced reactivity of the *pro*-ΛHT mono-adduct. The *pro*-ΛHT mono-adduct has the 5′-phosphate projecting towards the *cis*-coordinated solvent molecule (if we assume an *anti* conformation for the 5′-GMP nucleotide) and can form H-bonds with the coordinated water molecule, thus reducing its reactivity towards substitution by an incoming nucleophile. Therefore, in the case of (*R*,*R*)-**Me$_4$DACH** the reactivity of the *pro*-ΔHT mono-adduct will appear to be greater than expected if the reactivity of the *pro*-ΛHT mono-adduct is reduced. Moreover, in the case of (*S*,*S*)-**Me$_4$DACH** a reduced reactivity of the *pro*-ΛHT mono-adduct will result in a greater reactivity of the inherently more stable and less reactive *pro*-ΔHT mono-adduct (H8 atom of **G** on the same side of pseudo-axial *cis*-N–Me). The above hypothesis is also in accord with the smaller rate of formation of the bis-adduct observed for 5′-GMP than for 3′-GMP.

The HH rotamer has not been detected either in the formation reaction or at equilibrium. The absence of the HH rotamer, particularly during the formation reaction, was rather unexpected since in a previous investigation using the **Bip** carrier ligand (**Bip** = 2,2′-bipiperidine), it was demonstrated that the HH rotamer was formed in *ca.* 50% yield, the statistically expected value.[18] A possible explanation for the lack of formation of the HH rotamer in the present case is that the steric bulk created by the alkyl substituents on the coordinated nitrogens forces the two nucleobases to be closer to one another and to interact more strongly. Therefore, a dipolar coupling between the coordinated and the incoming purines could favour the HT rotamers over the HH rotamer even in the formation step.

Conclusions

Several important points have emerged from a comparison between fully substituted **Me$_4$DACH** substrates and previously investigated **CCC** systems having equal configurations on the carbon atoms bridging the two nitrogens.

First: The **Me$_4$DACH** ligand, similarly to **CCC** ligands, can induce a preference for an HT conformer which has Λ or Δ conformation for *R*,*R* or *S*,*S* configuration of the asymmetric carbons of the diamine, respectively. Such a preference stems from the major rotamer having a slightly greater canting of the "6-in" conformer favoured by the chirality of the carrier ligand (the H8 atoms of the guanines on the side of pseudo-axial N–Me groups with respect to the platinum coordination plane). Moreover, the difference in canting between the two HT rotamers is small; therefore the difference in concentration is also small and can be inverted by other factors such as 5′-phosphate-N1H *cis*-**G** H-bond formation.

Second: The absence of residual protons on the *cis*-coordinated nitrogens of **Me$_4$DACH** forces the 5′-phosphate to direct its H-bonding potential towards the other ligand in *cis* position (the coordinated water molecule in the mono-adduct and the second molecule of nucleotide in the bis-adduct). As a consequence, the *pro*-ΛHT conformer, having the 5′-phosphate directed towards the *cis*-coordinated water molecule (assuming an *anti* conformation of the nucleotide), is less reactive in both the (*R*,*R*) and (*S*,*S*)-**Me$_4$DACH** systems. Likewise the HT conformer of the bis-adduct in which the 5′-phosphate is directed towards the *cis*-nucleotide (the ΛHT rotamer) increases in stability. In the case of (*S*,*S*)-**Me$_4$DACH**, the 5′-phosphate-N1H *cis*-**G** interaction renders the ΛHT conformer more favoured notwithstanding the destabilisation of the HT rotamer having the H8 atoms of the guanines on the same side of the pseudo-equatorial N–Me's.

Third: Unlike the 5′-phosphate, the 3′-phosphate-N1H *cis*-**G** interaction does not appear to give any significant contribution to the stability of the ΔHT rotamer. The sterically demanding **Me$_4$DACH** ligand could constrain the two *cis*-nucleobases in a rather rigid conformation, thus preventing the formation of 3′-phosphate-N1H *cis*-**G** H-bond interactions. The negligible contribution of the 3′-phosphate to the stability of the ΔHT rotamer is accompanied by a significant role in promoting the reactivity of the mono-adduct, particularly that of the *pro*-ΔHT conformer. An anchimeric assistance of the 3′-phosphate to the release of the *cis*-coordinated water molecule and/or to the entering of the second molecule of nucleotide appears to be operating.

In conclusion this investigation has allowed the observation of specific interligand interactions in the coordination sphere of platinum complexes with nucleobases which were not observed with different carrier ligands comprising **CCC** ligands.

Experimental

All solvents were purchased from Aldrich Chemical Company and used as received. 5′-GMP, 3′-GMP and 9-EtG (Sigma) were used as received. Zeise's salt was prepared from potassium tetrachloroplatinate and ethylene gas as previously described.[24]

Syntheses

(*R*,*R*)-*N*,*N*,*N*′,*N*′-Tetramethyl-1,2-diaminocyclohexane, (*R*,*R*)-Me$_4$DACH·2HCl·H$_2$O. The optically pure (*R*,*R*)-1,2-diaminocyclohexane·2HCl, (*R*,*R*)-**DACH**·2HCl, (1.03 g, 5.5 mmol) was methylated following the procedure reported by Mok and coworkers.[25] (Yield 1.2 g, 89%), $[a]_D = -17.0°$ (*c* 4, H_2O). (Found: C, 45.4; H, 10.0; N, 10.3%. $C_{10}H_{26}Cl_2N_2O$ requires C, 45.9; H, 10.0; N, 10.7%). $\delta_H(D_2O)$ 1.43, 1.71, 1.88, and 2.24 (each signal integrates for 2H, m, methylene protons), 2.94 (12H, s, N–Me), 3.77 (2H, m, C*H*N).

(*S*,*S*)-*N*,*N*,*N*′,*N*′-Tetramethyl-1,2-diaminocyclohexane, (*S*,*S*)-Me$_4$DACH·2HCl·H$_2$O. The compound was prepared by the same procedure used for the synthesis of the *R*,*R* enantiomer. (Yield 88%), $[a]_D = +16.5°$ (*c* 4, H_2O). (Found: C, 45.5; H, 9.9; N, 10.5%. $C_{10}H_{26}Cl_2N_2O$ requires C, 45.9; H, 10.0; N, 10.7%). $\delta_H(D_2O)$ 1.41, 1.69, 1.87, and 2.30 (each signal integrates for 2H, m, methylene protons), 2.94 (12H, s, N–Me), 3.74 (2H, m, C*H*N).

(*R*,*R*)-Me$_4$DACH–PtCl$_2$. (*R*,*R*)-**Me$_4$DACH**·2HCl·H_2O (75.1 mg, 0.287 mmol) was dissolved in water, the solution was treated with a large excess of KOH (300 mg) and the free amine extracted with ether. The ether solution was treated with Zeise's salt (109.8 mg, 0.284 mmol) and the suspension kept under

stirring overnight. The yellow precipitate of (*R*,*R*)-**Me$_4$DACH**–$PtCl_2$ was transferred onto a filter and washed with abundant ether, to remove excess diamine, then with water, to remove KCl, and finally dried in a stream of dry air (Yield 100 mg, 80%). (Found: C, 27.7; H, 5.4; N, 6.1%. $C_{10}H_{22}Cl_2N_2Pt$ requires C, 27.5; H, 5.1; N, 6.4%). δ_H(DMSO-d_6) 1.07, 1.24, 1.58, and 2.05 (each signal integrates for 2H, m, methylene protons), 2.75 (6H, s, N–Me), 2.85 (6H, s, N–Me), 2.94 (2H, m, C*H*N).

(*S*,*S*)-Me$_4$DACH–PtCl$_2$. This compound was prepared following the same procedure described above for the *R*,*R* enantiomer (Yield 79%). (Found: C, 27.5; H, 5.2; N, 6.2%. $C_{10}H_{22}Cl_2N_2Pt$ requires C, 27.5; H, 5.1; N, 6.4%). δ_H(DMSO-d_6) 1.07, 1.24, 1.58, and 2.05 (each signal integrates for 2H, m, methylene protons), 2.75 (6H, s, N–Me), 2.85 (6H, s, N–Me), 2.94 (2H, m, C*H*N).

(*R*,*R*)-Me$_4$DACH–Pt(SO$_4$)·2H$_2$O. (*R*,*R*)-**Me$_4$DACH**–$PtCl_2$ (75.0 mg, 0.172 mmol) was suspended in water (50 ml) and treated with Ag_2SO_4 (56.0 mg, 0.179 mmol). The mixture was stirred overnight in the dark and the solution filtered to remove AgCl. The solvent was evaporated under vacuum and the solid residue extracted with MeOH. The solution was filtered to remove residual AgCl and the solvent evaporated to dryness. The pale yellow residue was the desired (*R*,*R*)-**Me$_4$DACH**–$Pt(SO_4)\cdot 2H_2O$ product (Yield 43 mg, 50%). (Found: C, 24.7; H, 5.1; N, 5.7%. $C_{10}H_{26}N_2O_6PtS$ requires C, 24.1; H, 5.3; N, 5.6%). δ_H(D_2O) 1.15, 1.46, 1.69, and 2.14 (each signal integrates for 2H, m, methylene protons), 2.79 (6H, s, N–Me), 2.81 (6H, s, N–Me), 3.05 (2H, m, C*H*N).

(*S*,*S*)-Me$_4$DACH–Pt(SO$_4$)·2H$_2$O. The synthesis of this compound was carried out as already described for the *R*,*R* enantiomer (Yield 45%). (Found: C, 24.3; H, 5.2; N, 5.6%. $C_{10}H_{26}N_2O_6PtS$ requires C, 24.1; H, 5.3; N, 5.6%). δ_H(D_2O) 1.15, 1.45, 1.69, and 2.14 (each signal integrates for 2H, m, methylene protons), 2.79 (6H, s, N–Me), 2.81 (6H, s, N–Me), 3.05 (2H, m, C*H*N).

Solution experiments

Stock solutions of **G** and **Me$_4$DACH**–$Pt(SO_4)\cdot 2H_2O$ (20–30 mM in D_2O) were prepared and adjusted to acidic pH* with diluted H_2SO_4 in D_2O (the asterisk indicates that no correction for deuterium was applied). The selected pH* was always *ca.* 3.0 except in the case of 9-EtG, for which a more acidic pH* (*ca.* 1.6) was required in order to ensure complete dissolution of the base in water. Because of the very poor coordination ability of O-donor ligands (such as sulfate) towards platinum, in water solution the sulfate is displaced by solvent molecules and the compound behaves as a 2 : 2 electrolyte. Aliquots of these stock solutions were transferred into a NMR tube in order to have a final **G**-to-platinum ratio slightly higher than two. The formation of **Me$_4$DACH**–Pt**G$_2$** complexes was monitored by UV-VIS, CD, and ^{1}H NMR techniques. For a given sample the time interval required for detection of the NMR, UV-VIS, and CD spectra never exceeded 15 min. The concentration of platinum complex in the NMR tube was in the range of 6–8 mM. The concentration of platinum complex in the solutions prepared for CD spectroscopy was between 0.04 and 0.05 mM.

Spectroscopy

^{1}H NMR spectra were recorded on a Bruker Advance dpx300 instrument. The number of scans per spectrum was at least 128 in order to increase the signal-to-noise ratio. CD and UV-VIS spectra were recorded on a Jasco J-810 spectropolarimeter in the range 200–350 nm. Each spectrum was the average of four different scans in order to increase the signal-to-noise ratio.

Acknowledgements

This work was supported by NIH Grant GM 29222 (to L.G.M.) and NATO CRG. 950376 (to L.G.M. and G.N.); MURST (PRIN 2001 no. 2001053898), CNR, and EC (COST Chemistry project D20/003/2000 and D20/001/2000) to G.N.

References

1 B. Rosenberg, L. Van Camp and T. Krigas, *Nature*, 1965, **205**, 698.
2 B. Rosenberg, L. Van Camp, E. B. Grimley and A. J. Thomson, *Biol. Chem.*, 1967, **242**, 1347.
3 B. Rosenberg, *Platinum Met. Rev.*, 1971, **15**, 42.
4 R. B. Weiss and M. C. Christian, *Drugs*, 1993, **46**, 360.
5 D. Lebwohl and R. Canetta, *Eur. J. Cancer*, 1998, **34**, 1522.
6 T. W. Hambley, *Coord. Chem. Rev.*, 1997, **166**, 181.
7 J. Reedijk, *Chem. Commun.*, 1996, 801.
8 E. R. Jamieson and S. J. Lippard, *J. Chem. Rev.*, 1999, **99**, 2467.
9 S. O. Ano, Z. Kuklenyik and L. G. Marzilli, in *Cisplatin: Chemistry and Biochemistry of a Leading Anticancer Drug*, ed. B. Lippert, Wiley-VCH, Weinheim, 1999, pp. 247–291.
10 L. G. Marzilli, J. S. Saad, Z. Kuklenyik, K. A. Keating and Y. Xu, *J. Am. Chem. Soc.*, 2001, **123**, 2764.
11 J. D. Orbell, M. R. Taylor, S. L. Birch, S. E. Lawton, L. M. Vilkins and L. J. Keefe, *Inorg. Chim. Acta*, 1988, **152**, 125.
12 U.-M. Ohndorf, M. A. Rould, Q. He, C. O. Pabo and S. J. Lippard, *Nature*, 1999, **399**, 708.
13 Y. Xu, G. Natile, F. P. Intini and L. G. Marzilli, *J. Am. Chem. Soc.*, 1990, **112**, 8177.
14 S. O. Ano, F. P. Intini, G. Natile and L. G. Marzilli, *J. Am. Chem. Soc.*, 1997, **119**, 8570.
15 L. G. Marzilli, F. P. Intini, D. Kiser, H. C. Wong, S. O. Ano, P. A. Marzilli and G. Natile, *Inorg. Chem.*, 1998, **37**, 6898.
16 S. O. Ano, F. P. Intini, G. Natile and L. G. Marzilli, *J. Am. Chem. Soc.*, 1998, **120**, 12017.
17 L. G. Marzilli, S. O. Ano, F. P. Intini and G. Natile, *J. Am. Chem. Soc.*, 1999, **121**, 9133.
18 S. O. Ano, F. P. Intini, G. Natile and L. G. Marzilli, *Inorg. Chem.*, 1999, **38**, 2989.
19 H. C. Wong, K. Shinozuka, G. Natile and L. G. Marzilli, *Inorg. Chim. Acta*, 2000, **297**, 36.
20 K. M. Williams, L. Cerasino, G. Natile and L. G. Marzilli, *J. Am. Chem. Soc.*, 2000, **122**, 8021.
21 J. S. Saad, T. Scarcia, K. Shinozuka, G. Natile and L. G. Marzilli, *Inorg. Chem.*, 2002, **41**, 546.
22 H. C. Wong, F. P. Intini, G. Natile and L. G. Marzilli, *Inorg. Chem.*, 1999, **38**, 1006.
23 H. C. Wong, R. Coogan, F. P. Intini, G. Natile and L. G. Marzilli, *Inorg. Chem.*, 1999, **38**, 777.
24 P. B. Chock, J. Halpern and F. E. Paulik, *Inorg. Synth.*, 1990, **28**, 349.
25 S. Y. M. Chooi, M. K. Tan, P. - H. Leung and K. F. Mok, *Inorg. Chem.*, 1994, **33**, 3096.